

APPLIED SCIENCES AND ENGINEERING

Hydrogel microenvironments for cancer spheroid growth and drug screening

Yunfeng Li¹ and Eugenia Kumacheva^{1,2,3*}

Multicellular cancer spheroids (MCSs) have emerged as a promising *in vitro* model that replicates many features of solid tumors *in vivo*. Biomimetic hydrogel scaffolds for MCS growth offer a broad spectrum of biophysical and biochemical cues that help to recapitulate the behavior of natural extracellular matrix, essential for regulating cancer cell behavior. This perspective highlights recent advances in the development of hydrogel environments for MCS growth, release, and drug screening. We review the use of different types of hydrogels for MCS growth, the effect of biophysical and biochemical cues on MCS fate, the isolation of MCSs from hydrogel scaffolds, the utilization of microtechnologies, and the applications of MCSs grown in hydrogels. We conclude with the discussion of new research directions in the development of hydrogels for MCS growth.

INTRODUCTION

Cancer remains one of the most life-threatening diseases worldwide. In 2015, nearly 15.2 million cancer cases have been diagnosed, and 8.8 million cancer patients died from cancer (1). Cancer prognosis depends on multiple factors, including the type and stage of the disease, patient genetics, age and gender, tumor environment, available treatment option, and patients' response to therapy. To conduct fundamental cancer research and develop effective therapies for cancer treatment, a variety of strategies are used that include analysis of clinical samples (biopsies), *in vivo* animal models, and *in vitro* models. Clinical samples are highly relevant to cancer patients; however, their utilization is limited by the heterogeneity and small sample size (2, 3). A promising strategy is a personalized patient-derived xenograft (PDX) model, which uses surgically obtained tumor sample of a cancer patient that is implanted and grown in immunodeficient mice (4, 5). Although *in vivo* models may provide a route toward personalized medicine for patients with cancer, these models are low-throughput, cost-intensive, and difficult to scale up. Because they are established in immunocompromised mice, the deficiency of an immune system may affect tumor development (6). Certain breast cancer cells have low engraftment rates or are not amenable to growth as PDX (7, 8).

In vitro models include cancer cell culture within porous scaffolds, hydrogels, paper stacks, or microfluidic (MF) channels to name just a few (9). These models, especially three-dimensional (3D) models, enable the exploration of a broad range of variables that affect tumor growth, invasion, and metastasis. They provide the capability of high-throughput drug screening that is not possible with *in vivo* animal models or clinical samples. Notably, the results obtained for *in vitro* models require validation for their biological relevance.

In particular, multicellular cancer spheroids (MCSs) have emerged as a promising *in vitro* model that replicates many features of solid tumors *in vivo*, including extracellular matrix (ECM) deposition between the cells, strong cell-cell junctions, and gradients in nutrient concentration (10–13). MCSs are 3D cancer cell aggregates with dimensions from tens of micrometers to ~1 mm (13–16). Growth of MCSs is carried out from cancer cell lines or primary cells, which may be combined with

fibroblasts, endothelial, or immune cells (17–20). Nonadhesive surfaces, spin flasks, or rotational bioreactors are used for MCS growth. With the development of microtechnologies, MCSs have also been formed in hanging droplets of culture medium, in micromolds, and in MF devices (21).

In many respects, MCSs mimic properties of metastatic microtumors that are formed by the spreading of cancer cells from the primary tumor by intravasation into the circulation and extravasation into the parenchyma of a distant organ (22–24). Because microtumors have dimensions that are too small for imaging by standard scanning techniques, an MCS model becomes particularly useful for the development of systemic therapies that either kill metastatic cells or lock them in the dormant state (22).

In vivo, tumors grow in ECMs composed of proteins, glycoproteins, proteoglycans, and polysaccharides (25). These ECM components offer a spectrum of biophysical properties and biochemical cues that are essential for regulating cancer cell behavior (26, 27). In particular, ECM stiffness, permeability, composition, spatial organization, and topography influence cancer cell proliferation, initiation, invasion, and metastasis, as well as tumor response to therapy (26, 28, 29). In addition, ECMs often have a filamentous structure rendered by fibrils of, for example, collagen, fibrin, or fibronectin, which provides structural support and specific distribution of cell adhesion receptors (27–30). ECMs also create spatially controlled cellular compartments (tumor capsules) that guide interactions between cancer cells and stroma cells (26). Cancer cells can remodel the surrounding ECMs by enzymatically degrading and rebuilding it, often making them behave as “protective” environments (31), which in turn affects tumor growth and response to therapies (26, 28).

The complexity and diversity of *in vivo* ECMs for tumor growth motivate the design and development of biomimetic environments for *in vitro* growth of 3D MCSs, especially from primary/patient cancer cells. Notably, some types of cancer cells that exhibit aggressive growth *in vivo* do not grow *in vitro*, where they lose the appropriate environment (2). Hydrogel-based artificial ECMs offer a spectrum of biophysical properties, the capability of their chemical modification, control over hydrogel structure and morphology, and the ability to design hydrogel shape and topography. Therefore, hydrogels have emerged as 3D biomimetic scaffolds for MCS growth and applications in fundamental cancer research and for studies of MCS response to different types of therapies (26, 29, 32).

Here, we highlight recent advances in the development of hydrogel environments for MCS growth, release, and drug screening. We start

Copyright © 2018
The Authors, some
rights reserved;
exclusive licensee
American Association
for the Advancement
of Science. No claim to
original U.S. Government
Works. Distributed
under a Creative
Commons Attribution
NonCommercial
License 4.0 (CC BY-NC).

¹Department of Chemistry, University of Toronto, 80 Saint George Street, Toronto, Ontario M5S 3H6, Canada. ²Department of Chemical Engineering and Applied Chemistry, University of Toronto, 200 College Street, Toronto, Ontario M5S 3E5, Canada. ³Institute of Biomaterials and Biomedical Engineering, University of Toronto, 4 Taddle Creek Road, Toronto, Ontario M5S 3G9, Canada.

*Corresponding author. Email: ekumache@chem.utoronto.ca

with the description of different types of hydrogel scaffolds that are currently used as environments for MCS growth and follow with the review of the effect of biophysical and biochemical cues on MCS fate. Subsequently, we discuss the methods of isolation of MCSs from hydrogel scaffolds for enhanced analysis and for their transfer to a different environment. Next, we outline the utilization of microtechnologies for MCS growth in hydrogels and review the applications of MCSs grown in hydrogel environments. We conclude with the discussion of challenges and research directions in the development of new types of hydrogels for growth and applications of cancer spheroids. This review highlights growth and applications of MCSs grown within 3D hydrogels. Growth of MCSs on 2D substrates or in the absence of hydrogels is the subject of several recent reviews (11, 13, 21).

3D HYDROGEL MICROENVIRONMENTS FOR MCS GROWTH

A hydrogel is a network of physically or chemically cross-linked polymer molecules that is inflated with an aqueous medium (33, 34). Hydrogels can be designed with a broad range of compositions, biophysical properties, and biological functions and can thus recapitulate many features of native ECMs. Therefore, biological and synthetic hydrogels have very promising applications for MCS growth, both for fundamental cancer research and for drug screening (26).

Protein-based hydrogels such as collagen (35–38), Matrigel (39–43), or fibrin (15) are commonly used for 3D cancer cell culture owing to their specific biophysical and cell-adhesive properties. Matrigel is recognized as a “golden standard” scaffold for MCS growth in vitro. It is extracted from Engelbreth-Holm-Swarm mouse sarcoma tumors and is composed primarily of laminin, type IV collagen, and entactin, as well as other constituents such as proteoglycans and growth factors (39). When polymerized, it forms a dense gel with relatively small pores (Fig. 1A) (44). Due to the presence of multiple growth factors, Matrigel promotes in vitro growth of MCSs from cell lines and primary cells (45–48) (growth of the latter is currently a challenge in man-made hydrogel scaffolds). Matrigel has been used for MCS growth from breast

cancer (Fig. 1B), colorectal cancer, and prostate cancer cell lines to name just a few (41, 49, 50). Many important findings have been made about MCSs grown in Matrigel. For example, it has been established that malignant breast cancer cells can be converted to the normal phenotype of the mammary epithelial cells by inhibiting β_1 integrin receptor or by down-regulating epidermal growth factor receptor (42).

Collagen, the most abundant fibrous protein component of ECM in mammals, plays a crucial role in tumor progression, invasion, and metastasis by promoting cell adhesion and migration (51–54). Therefore, 3D collagen gels are extensively used to mimic ECMs. For example, collagen type I hydrogels have been used to grow MCSs from osteosarcoma, breast cancer cells, human colorectal cancer cells, prostate cancer cell lines, and primary cancer cells from colorectal cancer patients (2, 35–38).

Polysaccharide hydrogels formed by hyaluronic acid (HA) (55, 56), agarose (57), or alginate (58, 59) have useful biophysical properties; however, they require additional chemical modification with, for example, arginylglycylaspartic acid (RGD) peptides (58) to introduce adhesion sites for mammalian cells. In contrast with Matrigel or collagen, polysaccharide hydrogels provide controllable and stable chemical and physical conditions for MCS growth, because their degradation is independent of cell-secreted proteolytic enzymes (58). Because of their mechanical stability, agarose and alginate hydrogels were used to determine the effect of stress imposed by growing MCSs on the hydrogels (57, 59).

Composite hydrogels with an interpenetrating network structure formed by polysaccharides and proteins offered control over mechanical properties of the hydrogel and provided cell adhesion ligands, thus facilitating MCS growth (60). Recently, MCSs have been efficiently grown from human ovarian cancer cells in alginate-collagen-agarose hydrogels (61). Alginate has also been combined with Matrigel to investigate the malignant progression of normal mammary epithelium mediated by changing hydrogel stiffness (40).

Biopolymer hydrogels offer a broad range of biochemical and biophysical properties for cell morphogenesis and function; however, the

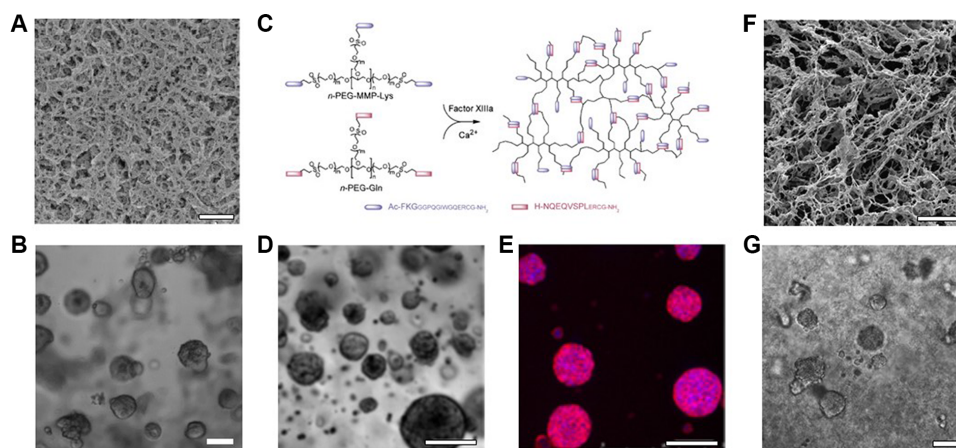


Fig. 1. MCS growth in hydrogel ECMs. (A) Scanning electron microscopy image of Matrigel. Scale bar, 1 μ m. (B) Phase-contrast microscopy image of MCSs grown from MCF-7 breast cancer cell lines in Matrigel for 14 days. Scale bar, 100 μ m. (C) PEG hydrogels are formed by a transglutaminase Factor XIIIa-catalyzed cross-linking reaction between two multi-arm PEG-peptide conjugates: *n*-PEG-MMP-Lys and *n*-PEG-Gln. Phase-contrast microscopy (D) and confocal microscopy (E) images of MCSs grown from OV-MZ-6 ovarian cancer cell lines in PEG hydrogels shown in (C). Scale bars, 100 μ m. Cell actin filaments were stained with rhodamine phalloidin (red), and the nuclei were stained with 4',6-diamidino-2-phenylindole (DAPI; blue). (F) Scanning electron microscopy image of the hydrogel formed from poly(*N*-isopropylacrylamide)-modified CNCs. Scale bar, 10 μ m. (G) MCS growth from MCF-7 breast cancer cell lines in hydrogels shown in (F). Scale bar, 100 μ m. Figures were reproduced with permission from Poincloux *et al.* (44) (A), Ehrbar *et al.* (66) (C), Loessner *et al.* (64) (D and E), and Li *et al.* (14) (F and G).

diversity of cues provided by natural scaffolds, their batch-to-batch variation, and uncontrolled degradation often limit the isolation of the effect of a specific ECM property on cancer cell fate and affect reproducibility of the results of comparative studies of cancer cell growth (26, 62). Synthetic hydrogel scaffolds carrying appropriate cell adhesion ligands and biodegradable cross-linkers may overcome these limitations by providing control over hydrogel composition and properties (26).

Synthetic hydrogels have been synthesized from linear or star poly(ethylene glycol) (PEG) molecules, which were cross-linked by photopolymerization of acrylate-PEG, by the click reaction between norbornene- and thiol-terminated PEG, or by the reaction between lysine- and glutamine-containing PEG (Fig. 1C) (63–66). Hydrogels formed from PEG have also been modified with integrin-binding RGD peptide molecules and matrix metalloproteinase degradable sites and used to grow MCSs from lung (63), ovarian (Fig. 1, D and E) (64), and brain cancer cell lines (65).

Another example of synthetic ECMs are hydrogels formed by the self-assembly of peptide molecules such as RADA16-I (AcN-RADARADARADARADA-CNH₂) (67). During the synthesis, specific ligands were attached to peptides to achieve desired biological functions of the hydrogel (68–70). These hydrogels contained entangled ~10-nm-thick fibers and had 5- to 200-nm-size pores (17). Peptide RADA16-I hydrogels (commercially available as BD PuraMatrix) (71) have been used to grow MCSs from ovarian cancer cell lines.

Unfortunately, synthetic preparation and purification of these hydrogels are cost- and labor-intensive, and they are not readily remodeled by cells. Furthermore, the morphology of synthetic hydrogel scaffolds often does not mimic the filamentous nature of natural ECMs (3, 62), which controls the spatial organization of the cell-adhesive ligands and mechanical signal transduction from cells to nanofibers of the ECM (30, 72, 73). Hybrid hydrogels derived from biological and synthetic constituents combine the best of both worlds: the advantages of natural polymers (that is, cell-adhesive ligands and filamentous structure) and synthetic polymers (that is, control of the biochemical and mechanical properties). For example, hydrogels have been formed from modified HA molecules (55, 74) by using the Michael-type addition reaction between acrylate-HA and thiolated-HA (75) or by oxime ligation between aldehyde-modified HA and bis(oxyamine)-PEG (76).

Another interesting example of hybrid scaffolds for MCS growth is a nanofibrillar hydrogel formed by rod-like cellulose nanocrystals (CNCs) carrying end-grafted molecules of a synthetic polymer poly(*N*-isopropylacrylamide) (14). As the shape and dimensions of CNCs are similar to those of collagen nanofibrils (77), the nanofibrillar structure of the hydrogel resembles the morphology of filamentous collagen and fibrin hydrogels (Fig. 1F). These hydrogels were used to culture breast cancer cells (Fig. 1G), with the MCS growth profiles being similar to those obtained in Matrigel.

BIOPHYSICAL AND BIOCHEMICAL CUES TO CONTROL THE MCS GROWTH

In vivo tumors grow in ECM environments with a broad spectrum of biochemical and biophysical properties (78, 79). To recreate microenvironments for tumor growth, the hydrogel of choice should replicate the properties of ECM, for example, its composition, structure, stiffness, and permeability. In particular, the role of hydrogel stiffness in MCS growth has been highlighted by showing that it affects the growth and phenotype of cancer cells. For example, MCS growth from individ-

ual murine B16-F1 melanoma cells has been explored for fibrin hydrogels with stiffness in the range from 90 to 1050 Pa (Fig. 2) (15). In stiff hydrogels, the size and the number of MCSs were markedly decreased (Fig. 2, C and D). In addition, MCSs grown in soft hydrogels had a high tumorigenicity when transferred *in vivo* (15). The matrix stiffness also affects the phenotype of cancer cells. Hepatocellular carcinoma cells encapsulated in a fat-like soft PEG-cross-linked collagen hydrogel formed malignant spheroids, whereas cells cultured in a liver-like, stiffer gel formed spheroids with suppressed malignancy (80). Although significant progress has been made on MCS growth in hydrogels with varying stiffness, the decoupling of the role of matrix stiffness and biochemical properties is still a challenge (81). Because hydrogel stiffness is generally controlled by varying polymer concentration, the resulting change in pore size (and thus in transport properties) and a varying density of cell adhesion sites can affect MCS growth.

Recently, the utilization of composite alginate-Matrigel hydrogels has enabled independent tuning of the matrix stiffness and composition (40). The stiffness of these hydrogels was modulated by controlling the degree of ionic cross-linking of alginate with Ca²⁺ ions at a constant polymer concentration, cell adhesion ligand density, and pore size. It was found that an increase of the matrix stiffness induced the malignant cell phenotype in mammary epithelium (40). Notably, with an increase in the concentration of basement membrane ligand (laminin-111), the acinar morphology in mammary epithelium was independent of the matrix stiffness.

Hydrogel composition, especially the presence of cell adhesion moieties, plays a crucial role in the MCS formation (58, 64). For example, in PEG hydrogels modified with RGD peptides (64), MCSs formed from the human epithelial ovarian cancer cell line proliferated faster and with a significantly higher spheroid number, in comparison with MCSs grown in the same hydrogels without RGD modification (64). Oral squamous cell carcinoma cells and brain and breast cancer cells also showed enhanced MCS growth within RGD-modified alginate hydrogels, in comparison with their culture in nonmodified alginate hydrogels (58).

These findings highlight the importance of controlling the interplay between the ECM stiffness and composition for the regulation of cell phenotype. They also provide insight needed for the development of strategies that may suppress cancer cell growth *in vivo*.

ISOLATION OF MCSs FROM HYDROGEL SCAFFOLDS

Postgrowth release of MCSs from hydrogel scaffolds is highly desirable for their analysis at the cellular and molecular levels (15, 33, 49), as well as MCS transfer *in vivo* to study their tumorigenic ability (2, 82). Commonly used mechanical hydrogel disruption (15) and enzymatically or chemically mediated hydrogel lysis (33) may affect MCS integrity. Photodegradation of the hydrogel is an alternative method for MCS liberation; however, ultraviolet irradiation may be harmful for the encapsulated cells (83).

The utilization of temperature-responsive hydrogels that liquefy at a reduced, yet physiologically appropriate, temperature offers a promising alternative to MCS release from the hydrogel matrix (84–88). The use of a hydrogel scaffold formed by CNCs tethered with poly(*N*-isopropylacrylamide) molecules enabled MCS growth at 37°C and their subsequent release by hydrogel dissolution at the temperature below the lower critical solution temperature of poly(*N*-isopropylacrylamide) (Fig. 3A) (14). Upon release, the MCSs did not exhibit noticeable dissociation (Fig. 3, B and C). The MCSs exhibited similar morphologies and size distribution before and after the release from the hydrogel.

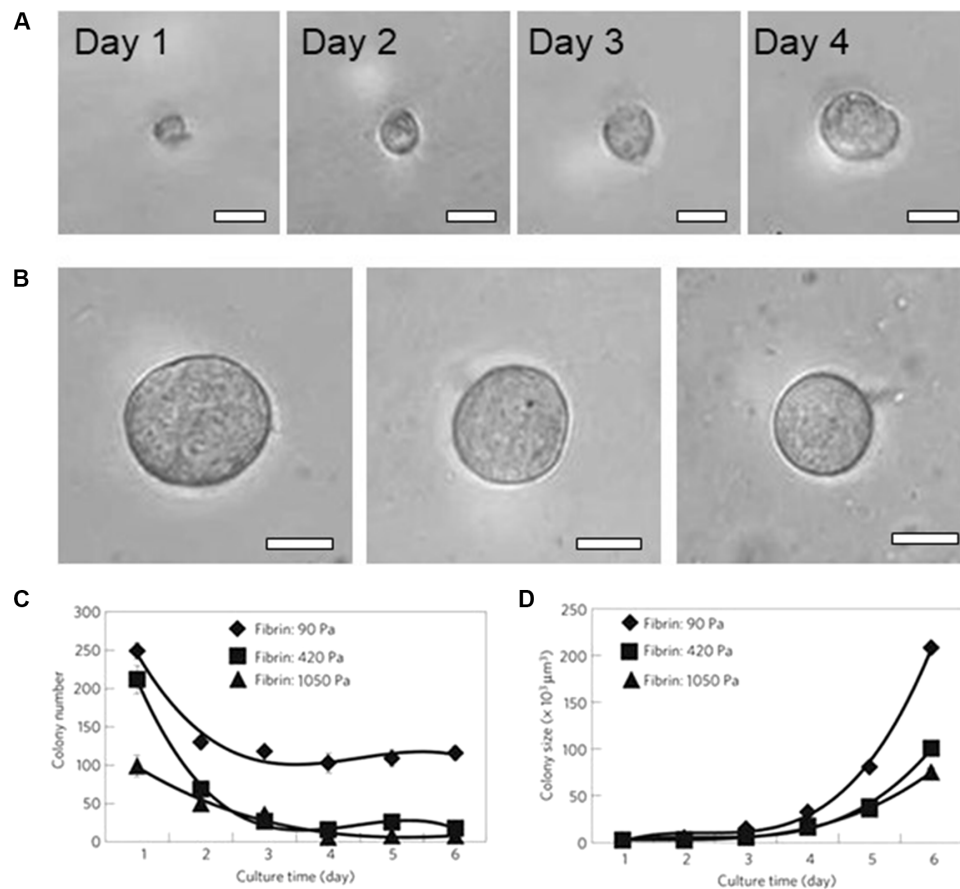


Fig. 2. Formation of MCSs in fibrin hydrogels with varying stiffness. (A) An individual B16-F1 cell grows into an MCS in fibrin gel with stiffness of 90 Pa within 4 days. (B) MCSs formed after 5-day culture from an individual B16-F1 cell in fibrin hydrogels with stiffness of 90 Pa (left), 420 Pa (middle), and 1050 Pa (right). Scale bars, 50 μm (A and B). (C) Variation in the MCS number with cell culture time in the fibrin hydrogels. (D) Increase in MCS size plotted as a function of culture time, plotted for hydrogels with different stiffness. The stiffness of 3D fibrin gels with concentrations of 1, 4, and 8 mg ml^{-1} is 90, 420, and 1050 Pa, respectively. Figures were reproduced with permission from Liu *et al.* (15) (A to D).

After the release, the MCSs were encapsulated in fibrin gel for further growth, thereby modeling the tumorigenic properties of MCSs implanted *in vivo*. Temperature-mediated MCS release offered (i) enhanced optical characterization of MCSs, due to reduced light scattering by the fibrous hydrogel (49, 89), and (ii) better MCS integrity, in comparison with that achieved by enzymatic or chemical hydrogel digestion (33, 90).

EMERGING MICROT�CHNOLOGIES FOR MCS GROWTH IN 3D MICROSCALE HYDROGELS

Advanced 3D *in vitro* cancer models have been recently developed by combining hydrogel-based cancer cell environments and microfabrication technologies. In comparison with conventional macroscopic 3D models, growth of MCSs in microscale hydrogels has the following advantages: (i) highly controllable MCS size, (ii) the ability to conduct high-content studies using small sample size, (iii) high reproducibility, and (iv) integration of MCS models with MFs to achieve MCS growth and high-throughput screening of drugs under close-to-physiological medium flow conditions (3).

Using hemispherical microwell arrays fabricated in polydimethylsiloxane, MCSs were formed by liver cancer cell line in the alginate hydrogel (91). The size of MCSs (controlled by the microwell dimensions)

was 150 to 400 μm . The viability and function of the spheroids were evaluated by releasing MCS-laden alginate microgels from the microwells and by measuring albumin secretion and urea synthesis using commercialized colorimetric assay kits (91).

Recently, growth of MCSs in an MF chip was implemented either in the absence of hydrogel scaffolds or by using conventional hydrogel scaffolds. For example, MCSs were grown from MCF-7 breast cell lines in the collagen hydrogel (92). The MCSs had a characteristic tumor tissue structure; however, the distribution in their dimensions suggested a potential difference in drug penetration, and thus the outcome of therapeutic treatment. Enhanced control of MCS dimensions was achieved by their compartmentalization in cell-laden hydrogel beads (93), hanging droplets (94–96), or in microwells (97–101). These experiments were conducted in the absence of hydrogels or without controlling hydrogel properties. In particular, uniformly sized MCSs formed from mouse colon carcinoma in alginate microcapsules that were generated by droplet MFs (59). Parallel streams of cell suspension in sorbitol solution, a solution of sorbitol, and sodium alginate solution were supplied to the MF droplet generator (Fig. 4A). A jet of the mixed suspension broke up periodically to generate cell-laden precursor droplets, which gelled off-chip in a calcium bath. Growth of MCSs was monitored in the alginate microcapsules (Fig. 4B) (59).

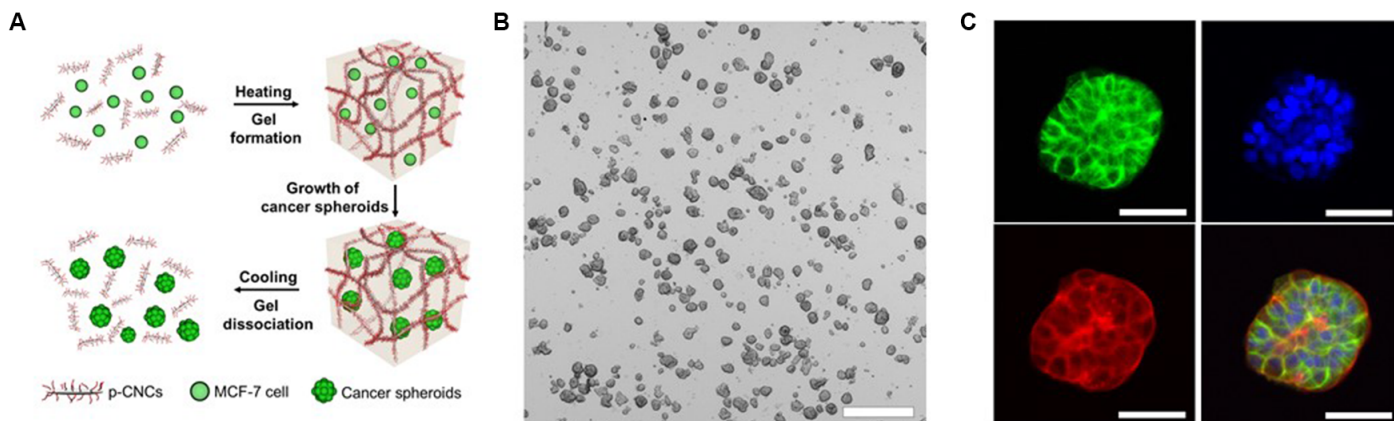


Fig. 3. MCF-7 release from p-CNC hydrogel. (A) Schematic of encapsulation, growth, and release of MCF-7 MCSs from the hydrogel formed by poly(*N*-isopropylacrylamide)-modified CNCs. (B) Phase-contrast microscopy images of MCF-7 MCSs released from the hydrogel as in (A) after 15-day culture. Scale bar, 500 μ m. (C) Immunostaining of the representative MCF-7 MCS released from the hydrogel as in (A) by Alexa Fluor 488 E-cadherin rabbit monoclonal antibody (green), DAPI (blue), Alexa Fluor 568 phalloidin (red), and the merged fluorescence image of the MCS. Scale bars, 50 μ m. Figures were reproduced with permission from Li *et al.* (14) (A to C).

Bioprinting has emerged as a very promising approach to *in vitro* 3D cancer models owing to its ability to create complex 3D architectures (102). Uniformly sized arrays of MCSs grown from breast and prostate cancer cell lines were formed by injecting cell-laden droplets in a collagen hydrogel in a 96-well plate (37). The MCS size and position were precisely controlled, which enabled automated imaging of the MCSs by using high-throughput imaging instrumentation (Becton Dickinson Pathway 855). MCSs from freshly isolated mouse breast (Fig. 4C) and human sarcoma (chondrosarcoma or osteosarcoma) biopsy material were prepared by this method, thereby indicating the potential for personalized cancer models (37).

APPLICATIONS OF MCSs GROWN IN HYDROGELS

Fundamental cancer cell biology research

Because MCSs grown in biomimetic hydrogels recapitulate many features of tumors formed *in vivo*, they serve as a useful *in vitro* model for fundamental research in cancer biology. An exemplary application of MCS models is the exploration of the angiogenic capability of cancer cells (58). For example, MCSs formed by oral squamous cell carcinoma cells in 3D alginate hydrogel were used to explore the angiogenic capacity of cancer cells in a specific environment. It was found that secretion of interleukin-8, a chemokine ligand playing an important role in tumor vascularization, was up-regulated in the alginate hydrogel modified with RGD peptide, in comparison with a nonmodified alginate hydrogel (58).

Recently, there has been an interest in the growth of tumorigenic cells, which are believed to cause cancer relapse. Growth of MCSs within hydrogels provided the ability to grow tumorigenic cells (13, 15, 103). For example, MCSs from multiple cancer cell lines or primary cancer cells were grown in fibrin hydrogels (15). Injection of as little as 10 cells that were dissociated from these MCSs in immunodeficient mice led to the formation of solid tumors at the injection site or at a distant organ (lungs) more efficiently than from cancer cells cultured on conventional rigid dishes or on soft gels.

Metastasis causes ~90% of all cancer-caused deaths (62); however, its mechanism is underinvestigated. Recently, using MCSs grown in hydrogels, invasion behavior and metastasis of cancer cells were studied systematically (72, 104, 105). MCSs from primary human mammary carcinoma were cultured in collagen and Matrigel (72, 104). MCSs in-

vaded the collagen hydrogel with protrusions and disseminated cells, whereas in Matrigel, MCSs were either indolent or grew collectively without protrusions (104). Moreover, to decouple factors that regulate cancer cell invasion and metastasis, MCSs from breast cancer cell lines were cultured in nanofibrillar collagen hydrogels with varying stiffness and pore size. It was found that the size of pores (controlled by the nanofibrillar gel structure), rather than viscoelastic gel properties, determined the invasion activity of the cells (72). The optimized cell invasion was observed in the hydrogels with a pore size of ~8 μ m, as well as suitable spatial organization of adhesion ligands in the nanofibrillar hydrogel; however, the mechanism of cancer invasion was not studied in detail. Cancer cell invasion was also studied using MCSs formed from malignant mammary epithelial cells in hybrid Matrigel/PEG hydrogels, in which PEG was tethered with the RGD peptide-conjugated α -cyclodextrin. Stronger cell invasion was observed in the hydrogels with an intermediate RGD peptide concentration (0.25%, w/v) and low stiffness (~100 Pa), whereas the same hydrogel without modification with RGD did not promote cell invasion (105). Stronger cell invasion in the RGD-modified hydrogels could be caused by the hydrogel network displacement driven by cell-mediated forces, with the assistance of cell adhesion.

Drug screening

MCSs grown in biomimetic hydrogels serve as a better model for the evaluation of drug efficacy than MCSs formed in the absence of hydrogels (13, 16, 106). Currently, MCSs grown in biomimetic hydrogels have not been extensively used for drug screening, mostly because of the labor-intensive hydrogel synthesis and challenges in the characterization of MCSs embedded in the hydrogels (17). Nevertheless, it has been established that after drug treatment, the structure and cell membranes in the MCSs grown in the collagen hydrogel were deteriorated, in comparison with control samples (Fig. 5, A and B) (107). Several recent studies showed that MCSs cultured in collagen hydrogel exhibited greater resistance to drugs than MCSs cultured in hydrogel-free conditions (106, 108), presumably because hydrogels acted as a barrier that slowed down drug diffusion and reduced the number of drug molecules reaching the MCS due to their binding to the hydrogel (13). Similarly, the response of MCSs to anticancer drugs such as doxorubicin and paclitaxel was weaker for the MCSs grown in the collagen hydrogel than that for

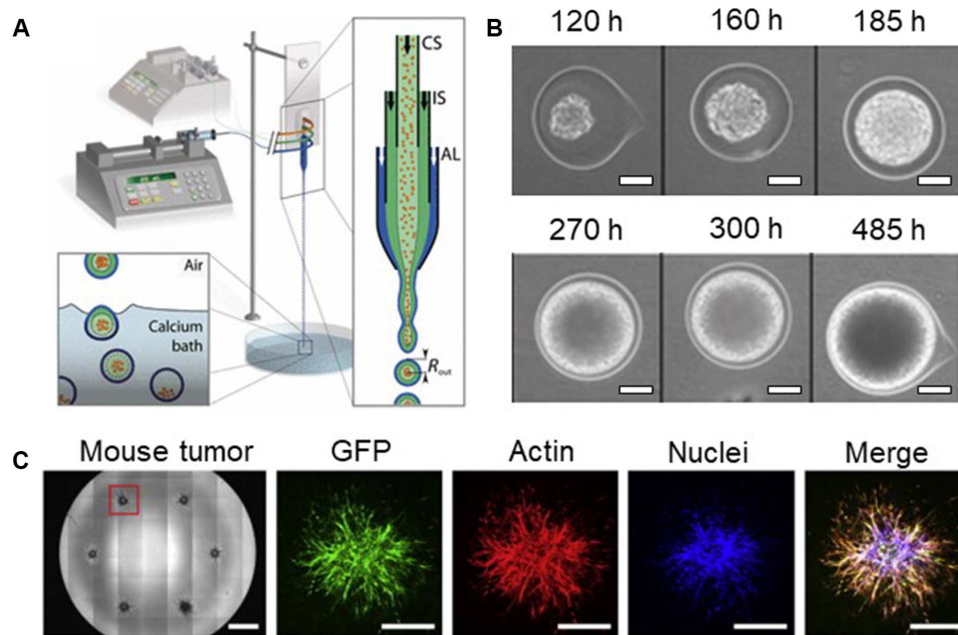


Fig. 4. Emerging microtechnologies for MCS growth in 3D microscale hydrogels. (A) Schematic of the MF platform for MCS formation, which is composed of an external fluidic injection system, coextrusion microdevice, and off-chip gelation bath. An enlarged view of the chip (right) shows the three-way configuration, with cell suspension (CS), intermediate solution (IS), and alginate solution (AL), respectively, flowing into the coaligned capillaries. The inlets of the chip are connected to three syringes controlled by two syringe pumps. The compound liquid microdroplets fall into a 100 mM calcium bath. Calcium-mediated gelation of the alginate shell freezes the structure of the capsule, and cells remain encapsulated. (B) Growth of a representative spheroid encapsulated in alginate capsule. Time on top of the images is recorded from encapsulation. Scale bars, 50 μm . (C) Bright-field images (left) of MCSs in a 96-well plate by bioprinting. Individual spheroid obtained from 4T1-green fluorescent protein (GFP) orthotopic mouse breast tumor. Scale bars, 1 mm (left image) and 500 μm (fluorescent images). Figures were reproduced with permission from Alessandri *et al.* (59) (A and B) and Truong *et al.* (37) (C).

the MCSs grown by 2D cell culture (107). To study the efficacy of therapeutic treatment of tumors in ECMs with varying stiffness, MCSs formed from breast cancer cells were encapsulated in collagen hydrogels with stiffness in the range from 300 to 6000 Pa and treated with paclitaxel (109). In soft hydrogels, paclitaxel-induced apoptosis of cancer cells was stronger than that for MCSs grown in stiffer matrices.

Furthermore, MCSs cultured in the collagen hydrogel were used to evaluate the therapeutic outcome of the different drug delivery methods (35). In particular, MCSs grown from breast cancer cells exhibited significantly stronger reduction in size upon treatment with polymer nanoparticles (NPs) loaded with paclitaxel, in comparison with MCSs treated with free paclitaxel (Fig. 5C). The decrease in the MCS size in response to the treatment with paclitaxel was similar for both the low and high drug doses, that is, 100 and 1000 ng/ml, respectively (35). To uncover the mechanism of drug uptake, MCSs formed by prostate cancer cells in the HA hydrogel were treated with free doxorubicin and doxorubicin-loaded polymer NPs (110). A stronger therapeutic effect was observed for doxorubicin-loaded NPs for MCSs cultured in the HA hydrogel than that for the free doxorubicin, which was caused by the internalization of drug-loaded NPs into tumor cells and subsequent release of doxorubicin in the cell interior.

The MCS models were also used to explore NP transport in tumor tissue for the optimization of NP size, shape, and surface chemistry for drug delivery and in vivo imaging (92, 111–114). Recently, a tumor-on-a-chip model was developed by introducing a Matrigel-surrounded MCS formed by melanoma cell lines (Fig. 5D) (114). It was found that the penetration of gold NPs into the tissue or Matrigel was controlled by the NP size (Fig. 5E) and that NP retention was improved by their

surface modification with the targeting receptors. The role of the flow conditions on NP delivery in the MCS was limited to their accumulation at the tissue periphery and did not affect their penetration depth (Fig. 5F) (114).

CONCLUSIONS AND PERSPECTIVES

Studies of MCSs formed in biomimetic hydrogels advance fundamental cancer research and provide deeper insight into the therapeutic tumor treatment. Man-made hydrogels with a broad spectrum of properties are constantly evolving in an effort to match the complexity of native tissues, and a large number of biological, synthetic, and hybrid hydrogels for MCS growth have been already developed (9). Further work should focus on the more accurate mimicking of in vivo environments for tumor growth, enhanced understanding of the role of the environment on cancer cell fate, and validation of the results obtained with MCS in vitro models. From this perspective, synthesizing or assembling “another gel” that acts comparably to, for example, Matrigel, cannot be considered as a significant advancement. Fundamental questions to be addressed include the effect of hydrogel properties on cancer initiation, cancer invasion, metastasis, and response to therapy. For example, the effects of hydrogel biophysical properties (for example, stiffness and permeability) and composition on cancer fate have to be decoupled. Although the importance of ECM (hydrogel) stiffness on the MCS growth is established, the majority of studies have focused on the hydrogel elasticity and overlooked the role of its viscoelasticity. It was recently found that viscoelastic properties of hydrogel substrates with stress relaxation can stimulate the spreading of osteosarcoma cells to a greater extent

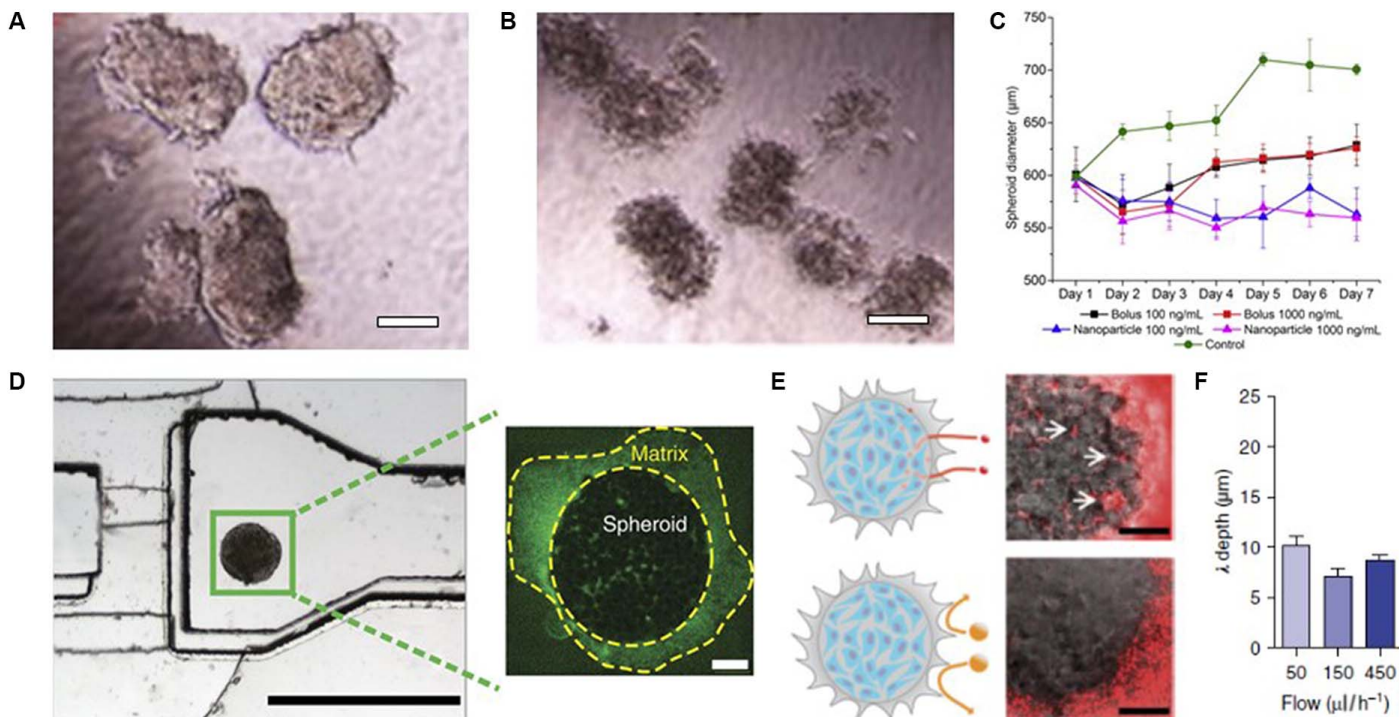


Fig. 5. MCSs in the hydrogels as models for drug screening and NP transport. Morphology of MCSs formed by coculture of the human hepatocellular liver carcinoma cell line HepG2 and fibroblasts in collagen hydrogel without (A) and with (B) 10 μM doxorubicin treatment for 4 days. Scale bars, 100 μm. (C) Change in diameter of MCSs (breast cancer cell line MDA-MB-231) in the collagen hydrogels, plotted as a function of duration of the paclitaxel treatment. The drug was delivered via bolus dose or NPs for 24 hours. (D) Image of the MF device (left) with MCS (MDA-MB-435 melanoma cell line) in Matrigel, which was used to study NP transport in the tumor tissue model. Scale bar, 1000 μm. The spheroid (right) stained with anti-Laminin-FITC (fluorescein isothiocyanate). Scale bar, 100 μm. (E) Schematic (left) and image (right) of 40 (top) and 110 nm (bottom) fluorescent PEG-Au NPs administered for 1 hour at the flow rate of 50 ml/h. The 40-nm NPs entered the MCS and accumulated in the interstitial spaces (arrows in top image), and the 110-nm NPs were excluded from the MCS. Scale bars, 100 μm. Images in (E) represent an overlay of fluorescence (excitation, 633 nm; emission, 650 to 700 nm) and differential interference contrast images. (F) NP penetration depth in MCSs treated with 40-nm PEG-Au NPs at various flow rates. Figures were reproduced with permission from Yip *et al.* (107) (A and B), Charoen *et al.* (35) (C), and Albanese *et al.* (114) (D to F).

than purely elastic hydrogel substrates with the same initial elastic modulus (115). The role of hydrogel structure, that is, its filamentous nature, anisotropy, and hierarchical architecture, is underinvestigated, and it is desirable to examine it with respect to each particular type of cancer. Chemical functionalization of man-made hydrogels for MCS growth can better replicate a biochemical environment for tumor growth. This approach was used by attaching cell-cell signaling factors and components of pancreatic tissue-specific ECM to poly(ethylene glycol)-*co*-poly-L-lysine hydrogel beads surrounding pancreatic cells (116), and it can be used in cancer research.

Other factors that should be considered for hydrogel improvement include the ease and the cost of its preparation, the fine-tuning of gelation time, and the hydrogel stability.

It is established that degradation and remodeling of ECM by cancer cells may result in ECM heterogeneity and thus lead to spatial variation in density and network organization. Alignment and orientation of collagen I fibers perpendicular to the tumor boundary have been associated with cancer relapse after surgical excision and preferential migration of breast cancer cells along the aligned fibers (117, 118). To understand the role of dynamic niches on tumor progression, further efforts should focus on the use of hydrogels with structures characteristic for specific types of cancer, for example, hydrogels with fibrillar structures and well-defined spatial nanofiber alignment.

During tumor development, the adjacent ECM is degraded and remodeled by cancer cells. The ECM niche, in turn, influences tumor pro-

gression and response to therapy; however, in general, only initial hydrogel properties are characterized, and the change in the density, stiffness, or permeability of hydrogels during the course of MCS growth is not considered. Thus, advanced methods are required to characterize changes in the hydrogel adjacent to the MCS.

After MCS growth and therapeutic treatment, it is imperative to release them from the hydrogel matrix for the analysis using flow cytometry or molecular characterization by the reverse transcription polymerase chain reaction or by Western blots. In addition, because nanofibrillar gels may scatter light in the visible part of the spectrum, MCS release can facilitate their imaging by optical microscopy. Commonly used methods for MCS release use enzymatically or chemically mediated hydrogel lysis, which may affect MCS integrity. Advanced hydrogel-based ECMs leading to MCS release under mild conditions are highly desired.

Currently, well-established cancer cell lines are routinely used to grow MCSs; however, during culture and passage, cell lines acquire changes in gene expression and morphology and lose some characteristics of primary tumors (119, 120). In contrast, primary cells would better retain the properties of the original tumor (120, 121), and MCS growth from primary cells would have a stronger similarity with tumor tissue in both the composition and the architecture. Presently, this process is challenging: Conditions for primary cancer cell growth are not optimized and cell viability is low (121). Growth of MCSs derived from the biopsy of cancer patients offers the approach to “precision cancer

medicine,” a personalized therapeutic tool that predicts the outcome of therapeutic treatment for a specific patient. Screening of drugs on these MCSs can provide useful information that would enable clinicians to make a better decision about the most efficient clinical management strategy for a specific patient. In addition, this may open up opportunities for applying novel agents for patients that cannot be cured with standard chemotherapy drugs (47, 122). Hydrogels that support MCS growth from cancer cells that are isolated from patient tumor tissues are in high demand, especially when these hydrogels are designed for studies of a specific type of cancer. Although MCSs have been grown from primary cancer cells in collagen and Matrigel (2, 46, 47), the full potential of these MCSs in basic cancer research and drug screening is not completely realized (123). The utilization of genetic manipulation tools, for example, CRISPR-Cas9, to capture characteristic molecular aspects of MCSs grown in different hydrogels may prove useful for accurately reproducing the properties of tumor environments in vivo.

Growth of MCSs in 3D microscale hydrogels has already advanced basic cancer research and paved the way for the discovery of anticancer drugs. In particular, a tumor-on-a-chip approach implemented by combining MCSs and MFs is rapidly developing to study cancer initiation and progression and screen anticancer therapies in a high-throughput fashion. Currently, tumor-on-a-chip models have a limited use outside academic laboratories due to the potential complexity of the MF devices and the lack of robustness of hydrogels under continuous medium flow. Covalently cross-linked hydrogels are needed for these applications, as well as simple MCS culture protocols and automated imaging and analytic techniques.

REFERENCES AND NOTES

1. GBD 2015 Mortality and Causes of Death Collaborators, Global, regional, and national life expectancy, all-cause mortality, and cause-specific mortality for 249 causes of death, 1980–2015: A systematic analysis for the Global Burden of Disease Study 2015. *Lancet* **388**, 1459–1544 (2016).
2. J. Kondo, H. Endo, H. Okuyama, O. Ishikawa, H. Iishi, M. Tsujii, M. Ohue, M. Inoue, Retaining cell–cell contact enables preparation and culture of spheroids composed of pure primary cancer cells from colorectal cancer. *Proc. Natl. Acad. Sci. U.S.A.* **108**, 6235–6240 (2011).
3. K. E. Sung, D. J. Beebe, Microfluidic 3D models of cancer. *Adv. Drug Deliv. Rev.* **79–80**, 68–78 (2014).
4. C. L. Scott, M. A. Becker, P. Haluska, G. Samimi, Patient-derived xenograft models to improve targeted therapy in epithelial ovarian cancer treatment. *Front. Oncol.* **3**, 295 (2013).
5. S. J. Weroha, M. A. Becker, S. Enderica-Gonzalez, S. C. Harrington, A. L. Oberg, M. J. Maurer, S. E. Perkins, M. AlHilli, K. A. Butler, S. McKinstry, S. Fink, R. B. Jenkins, X. Hou, K. R. Kalli, K. M. Goodman, J. N. Sarkaria, B. Y. Karlan, A. Kumar, S. H. Kaufmann, L. C. Hartmann, P. Haluska, Tumorgrafts as in vivo surrogates for women with ovarian cancer. *Clin. Cancer Res.* **20**, 1288–1297 (2014).
6. L. R. Kelland, “Of mice and men”: Values and liabilities of the athymic nude mouse model in anticancer drug development. *Eur. J. Cancer* **40**, 827–836 (2004).
7. J. R. Whittle, M. T. Lewis, G. J. Lindeman, J. E. Visvader, Patient-derived xenograft models of breast cancer and their predictive power. *Breast Cancer Res.* **17**, 17 (2015).
8. Y. S. DeRose, G. Wang, Y.-C. Lin, P. S. Bernard, S. S. Buys, M. T. W. Ebbert, R. Factor, C. Matsen, B. A. Milash, E. Nelson, L. Neumayer, R. L. Randall, I. J. Stijleman, B. E. Welm, A. L. Welm, Tumor grafts derived from women with breast cancer authentically reflect tumor pathology, growth, metastasis and disease outcomes. *Nat. Med.* **17**, 1514–1520 (2011).
9. D. Rodenhizer, T. Dean, E. D’Arcangelo, A. P. McGuigan, The current landscape of 3D in vitro tumor models: What cancer hallmarks are accessible for drug discovery? *Adv. Healthc. Mater.* 10.1002/adhm.201701174 (2018).
10. R. M. Sutherland, Cell and environment interactions in tumor microregions: The multicell spheroid model. *Science* **240**, 177–184 (1988).
11. E. C. Costa, A. F. Moreira, D. Melo-Diogo, V. M. Gaspar, M. P. Carvalho, I. J. Correia, 3D tumor spheroids: An overview on the tools and techniques used for their analysis. *Biotechnol. Adv.* **34**, 1427–1441 (2016).
12. R.-Z. Lin, H.-Y. Chang, Recent advances in three-dimensional multicellular spheroid culture for biomedical research. *Biotechnol. J.* **3**, 1172–1184 (2008).
13. G. Mehta, A. Y. Hsiao, M. Ingram, G. D. Luker, S. Takayama, Opportunities and challenges for use of tumor spheroids as models to test drug delivery and efficacy. *J. Control. Release* **164**, 192–204 (2012).
14. Y. Li, N. Khuu, A. Gevorkian, S. Sarjinsky, H. Therien-Aubin, Y. Wang, S. Cho, E. Kumacheva, Supramolecular nanofibrillar thermoreversible hydrogel for growth and release of cancer spheroids. *Angew. Chem. Int. Ed. Engl.* **56**, 6083–6087 (2017).
15. J. Liu, Y. Tan, H. Zhang, Y. Zhang, P. Xu, J. Chen, Y.-C. Poh, K. Tang, N. Wang, B. Huang, Soft fibrin gels promote selection and growth of tumorigenic cells. *Nat. Mater.* **11**, 734–741 (2012).
16. A. I. Minchinton, I. F. Tannock, Drug penetration in solid tumours. *Nat. Rev. Cancer* **6**, 583–592 (2006).
17. X. Xu, M. C. Farach-Carson, X. Jia, Three-dimensional in vitro tumor models for cancer research and drug evaluation. *Biotechnol. Adv.* **32**, 1256–1268 (2014).
18. M. Upreti, A. Jamshidi-Parsian, N. A. Koonce, J. S. Webber, S. K. Sharma, A. A. A. Asea, M. J. Mader, R. J. Griffin, Tumor-endothelial cell three-dimensional spheroids: New aspects to enhance radiation and drug therapeutics. *Transl. Oncol.* **4**, 365–376 (2011).
19. Z. Lao, C. J. Kelly, X.-Y. Yang, W. T. Jenkins, E. Toorens, T. Ganguly, S. M. Evans, C. J. Koch, Improved methods to generate spheroid cultures from tumor cells, tumor cells & fibroblasts or tumor-fragments: Microenvironment, microvesicles and MiRNA. *PLOS ONE* **10**, e0133895 (2015).
20. S. Herter, L. Morra, R. Schlenker, J. Sulcova, L. Fahrni, I. Waldhauer, S. Lehmann, T. Reisländer, I. Agarkova, J. M. Kelm, C. Klein, P. Umana, M. Bacac, A novel three-dimensional heterotypic spheroid model for the assessment of the activity of cancer immunotherapy agents. *Cancer Immunol. Immunother.* **66**, 129–140 (2017).
21. X. Cui, Y. Hartanto, H. Zhang, Advances in multicellular spheroids formation. *J. R. Soc. Interface* **14**, 20160877 (2017).
22. J. J. Christiansen, A. K. Rajasekaran, Reassessing epithelial to mesenchymal transition as a prerequisite for carcinoma invasion and metastasis. *Cancer Res.* **66**, 8319–8326 (2006).
23. D. P. Taylor, J. Z. Wells, A. Savol, C. Chennubhotla, A. Wells, Modeling boundary conditions for balanced proliferation in metastatic latency. *Clin. Cancer Res.* **19**, 1063–1070 (2013).
24. R. A. Weinberg, The many faces of tumor dormancy. *Apms* **116**, 548–551 (2008).
25. J. H. Miner, The Extracellular Matrix: An Overview, in *Cell-Extracellular Matrix Interactions in Cancer*, R. Zent, A. Pozzi, Eds. (Springer, 2010), pp. 1–7.
26. L. Gu, D. J. Mooney, Biomaterials and emerging anticancer therapeutics: Engineering the microenvironment. *Nat. Rev. Cancer* **16**, 56–66 (2016).
27. L. G. Griffith, M. A. Swartz, Capturing complex 3D tissue physiology in vitro. *Nat. Rev. Mol. Cell Biol.* **7**, 211–224 (2006).
28. P. Lu, V. M. Weaver, Z. Werb, The extracellular matrix: A dynamic niche in cancer progression. *J. Cell Biol.* **196**, 395–406 (2012).
29. F. Klemm, J. A. Joyce, Microenvironmental regulation of therapeutic response in cancer. *Trends Cell Biol.* **25**, 198–213 (2015).
30. R. O. Hynes, The extracellular matrix: Not just pretty fibrils. *Science* **326**, 1216–1219 (2009).
31. A. M. Clark, S. E. Wheeler, D. P. Taylor, V. C. Pillai, C. L. Young, R. Prantil-Baun, T. Nguyen, D. B. Stolz, J. T. Borenstein, D. A. Lauffenburger, R. Venkataramanan, L. G. Griffith, A. Wells, A microphysiological system model of therapy for liver micrometastases. *Exp. Biol. Med.* **239**, 1170–1179 (2014).
32. H. J. Kong, D. J. Mooney, Microenvironmental regulation of biomacromolecular therapies. *Nat. Rev. Drug Discov.* **6**, 455–463 (2007).
33. S. R. Caliji, J. A. Burdick, A practical guide to hydrogels for cell culture. *Nat. Methods* **13**, 405–414 (2016).
34. J. Thiele, Y. Ma, S. M. C. Bruekers, S. Ma, W. T. S. Huck, 25th anniversary article: Designer hydrogels for cell cultures: A materials selection guide. *Adv. Mater.* **26**, 125–148 (2014).
35. K. M. Charoen, B. Fallica, Y. L. Colson, M. H. Zaman, M. W. Grinstaff, Embedded multicellular spheroids as a biomimetic 3D cancer model for evaluating drug and drug-device combinations. *Biomaterials* **35**, 2264–2271 (2014).
36. S.-Y. Jeong, J.-H. Lee, Y. Shin, S. Chung, H.-J. Kuh, Co-culture of tumor spheroids and fibroblasts in a collagen matrix-incorporated microfluidic chip mimics reciprocal activation in solid tumor microenvironment. *PLOS ONE* **11**, e0159013 (2016).
37. H. H. Truong, J. de Sonnevill, V. P. S. Ghotra, J. Xiong, L. Price, P. C. W. Hogendoorn, H. H. Spaik, B. de Water, E. H. J. Danen, Automated microinjection of cell-polymer suspensions in 3D ECM scaffolds for high-throughput quantitative cancer invasion screens. *Biomaterials* **33**, 181–188 (2012).
38. C. S. Szot, C. F. Buchanan, J. W. Freeman, M. N. Rylander, 3D in vitro bioengineered tumors based on collagen I hydrogels. *Biomaterials* **32**, 7905–7912 (2011).
39. G. Benton, I. Arnaoutova, J. George, H. K. Kleinman, J. Koblinski, Matrigel: From discovery and ECM mimicry to assays and models for cancer research. *Adv. Drug Deliv. Rev.* **79–80**, 3–18 (2014).

40. O. Chaudhuri, S. T. Koshy, C. Branco da Cunha, J.-W. Shin, C. S. Verbeke, K. H. Allison, D. J. Mooney, Extracellular matrix stiffness and composition jointly regulate the induction of malignant phenotypes in mammary epithelium. *Nat. Mater.* **13**, 970–978 (2014).
41. S. H. Lang, R. M. Sharrard, M. Stark, J. M. Villette, N. J. Maitland, Prostate epithelial cell lines form spheroids with evidence of glandular differentiation in three-dimensional Matrigel cultures. *Br. J. Cancer* **85**, 590–599 (2001).
42. V. M. Weaver, O. W. Petersen, F. Wang, C. A. Larabell, P. Briand, C. Damsky, M. J. Bissell, Reversion of the malignant phenotype of human breast cells in three-dimensional culture and in vivo by integrin blocking antibodies. *J. Cell Biol.* **137**, 231–245 (1997).
43. V. Härmä, J. Virtanen, R. Mäkelä, A. Happonen, J.-P. Mpindi, M. Knuutila, P. Kohonen, J. Lötjönen, O. Kallioniemi, M. Nees, A comprehensive panel of three-dimensional models for studies of prostate cancer growth, invasion and drug responses. *PLOS ONE* **5**, e10431 (2010).
44. R. Poincloux, F. Lizárraga, P. Chavrier, Matrix invasion by tumour cells: A focus on MT1-MMP trafficking to invadopodia. *J. Cell Sci.* **122**, 3015–3024 (2009).
45. R. Fridman, G. Giaccone, T. Kanemoto, G. R. Martin, A. F. Gazdar, J. L. Mulshine, Reconstituted basement membrane (matrigel) and laminin can enhance the tumorigenicity and the drug resistance of small cell lung cancer cell lines. *Proc. Natl. Acad. Sci. U.S.A.* **87**, 6698–6702 (1990).
46. S. F. Boj, C.-I. Hwang, L. A. Baker, I. C. Chio, D. D. Engle, V. Corbo, M. Jager, M. Ponz-Sarvisse, H. Tiriác, M. S. Spector, A. Gracanin, T. Oni, K. H. Yu, R. van Bostel, M. Huch, K. D. Rivera, J. P. Wilson, M. E. Feigin, D. Öhlund, A. Handy-Santana, C. M. Ardito-Abraham, M. Ludwig, E. Elyada, B. Alagesan, G. Biffi, G. N. Yordanov, B. Delcuze, B. Creighton, K. Wright, Y. Park, F. H. M. Morsink, I. Q. Molenaar, I. H. Borel Rinkes, E. Cuppen, Y. Hao, Y. Jin, I. J. Nijman, C. Iacobuzio-Donahue, S. D. Leach, D. J. Pappin, M. Hammell, D. S. Klimstra, O. Basturk, R. H. Hruban, G. J. Offerhaus, R. G. J. Vries, H. Clevers, D. A. Tuveson, Organoid models of human and mouse ductal pancreatic cancer. *Cell* **160**, 324–338 (2015).
47. C. Pauli, B. D. Hopkins, D. Prandi, R. Shaw, T. Fedrizzi, A. Sboner, V. Sailer, M. Augello, L. Puca, R. Rosati, T. J. McNary, Y. Churakova, C. Cheung, J. Triscott, D. Pisapia, R. Rao, J. M. Mosquera, B. Robinson, B. M. Faltas, B. E. Emerling, V. K. Gadi, B. Bernard, O. Elemento, H. Beltran, F. Demichelis, C. J. Kemp, C. Grandori, L. C. Cantley, M. A. Rubin, Personalized in vitro and in vivo cancer models to guide precision medicine. *Cancer Discov.* **7**, 462–477 (2017).
48. L. Huang, A. Holtzinger, I. Jagan, M. BeGora, I. Lohse, N. Ngai, C. Nostro, R. Wang, L. B. Muthuswamy, H. C. Crawford, C. Arrowsmith, S. E. Kalloger, D. J. Renouf, A. A. Connor, S. Cleary, D. F. Schaeffer, M. Roehrl, M.-S. Tsao, S. Gallinger, G. Keller, S. K. Muthuswamy, Ductal pancreatic cancer modeling and drug screening using human pluripotent stem cell- and patient-derived tumor organoids. *Nat. Med.* **21**, 1364–1371 (2015).
49. G. Y. Lee, P. A. Kenny, E. H. Lee, M. J. Bissell, Three-dimensional culture models of normal and malignant breast epithelial cells. *Nat. Methods* **4**, 359–365 (2007).
50. T. M. Yeung, S. C. Gandhi, J. L. Wilding, R. Muschel, W. F. Bodmer, Cancer stem cells from colorectal cancer-derived cell lines. *Proc. Natl. Acad. Sci. U.S.A.* **107**, 3722–3727 (2010).
51. K. M. Park, S. Gerecht, Polymeric hydrogels as artificial extracellular microenvironments for cancer research. *Eur. Polym. J.* **72**, 507–513 (2015).
52. M. Egeblad, M. G. Rasch, V. M. Weaver, Dynamic interplay between the collagen scaffold and tumor evolution. *Curr. Opin. Cell Biol.* **22**, 697–706 (2010).
53. M. J. Paszek, N. Zahir, K. R. Johnson, J. N. Lakin, G. I. Rozenberg, A. Gefen, C. A. Reinhart-King, S. S. Margulies, M. Dembo, D. Boettiger, D. A. Hammer, V. M. Weaver, Tensional homeostasis and the malignant phenotype. *Cancer Cell* **8**, 241–254 (2005).
54. D. M. Gilkes, P. Chaturvedi, S. Bajpai, C. C. Wong, H. Wei, S. Pitcairn, M. E. Hubbi, D. Wirtz, G. L. Semenza, Collagen prolyl hydroxylases are essential for breast cancer metastasis. *Cancer Res.* **73**, 3285–3296 (2013).
55. S. Pedron, E. Becka, B. A. C. Harley, Regulation of glioma cell phenotype in 3D matrices by hyaluronic acid. *Biomaterials* **34**, 7408–7417 (2013).
56. L. A. Gurski, A. K. Jha, C. Zhang, X. Jia, M. C. Farach-Carson, Hyaluronic acid-based hydrogels as 3D matrices for in vitro evaluation of chemotherapeutic drugs using poorly adherent prostate cancer cells. *Biomaterials* **30**, 6076–6085 (2009).
57. G. Helmlinger, P. A. Netti, H. C. Lichtenbeld, R. J. Melder, R. K. Jain, Solid stress inhibits the growth of multicellular tumor spheroids. *Nat. Biotechnol.* **15**, 778–783 (1997).
58. C. Fischbach, H. J. Kong, S. X. Hsiang, M. B. Evangelista, W. Yuen, D. J. Mooney, Cancer cell angiogenic capability is regulated by 3D culture and integrin engagement. *Proc. Natl. Acad. Sci. U.S.A.* **106**, 399–404 (2009).
59. K. Alessandri, B. R. Sarangi, V. V. Gurchenkov, B. Sinha, T. R. Kießling, L. Fetler, F. Rico, S. Scheuring, C. Lamaze, A. Simon, S. Geraldo, D. Vignjević, H. Doméjan, L. Rolland, A. Furfak, J. Bibette, N. Bremond, P. Nassoy, Cellular capsules as a tool for multicellular spheroid production and for investigating the mechanics of tumor progression in vitro. *Proc. Natl. Acad. Sci. U.S.A.* **110**, 14843–14848 (2013).
60. S. Pradhan, I. Hassani, J. M. Clary, E. A. Lipke, Polymeric biomaterials for in vitro cancer tissue engineering and drug testing applications. *Tissue Eng. Part B Rev.* **22**, 470–484 (2016).
61. S. Shin, M. Ikram, F. Subhan, H. Y. Kang, Y. Lim, R. Lee, S. Jin, Y. H. Jeong, J.-Y. Kwak, Y.-J. Na, S. Yoon, Alginate–marine collagen–agarose composite hydrogels as matrices for biomimetic 3D cell spheroid formation. *RSC Adv.* **6**, 46952–46965 (2016).
62. M. Alemany-Ribes, C. E. Semino, Bioengineering 3D environments for cancer models. *Adv. Drug Deliv. Rev.* **79–80**, 40–49 (2014).
63. B. J. Gill, D. L. Gibbons, L. C. Roudsari, J. E. Saik, Z. H. Rizvi, J. D. Roybal, J. M. Kurie, J. L. West, A synthetic matrix with independently tunable biochemistry and mechanical properties to study epithelial morphogenesis and EMT in a lung adenocarcinoma model. *Cancer Res.* **72**, 6013–6023 (2012).
64. D. Loessner, K. S. Stok, M. P. Lutolf, D. W. Hutmacher, J. A. Clements, S. C. Rizzi, Bioengineered 3D platform to explore cell–ECM interactions and drug resistance of epithelial ovarian cancer cells. *Biomaterials* **31**, 8494–8506 (2010).
65. C. Wang, X. Tong, F. Yang, Bioengineered 3D brain tumor model to elucidate the effects of matrix stiffness on glioblastoma cell behavior using PEG-based hydrogels. *Mol. Pharm.* **11**, 2115–2125 (2014).
66. M. Ehrbar, S. C. Rizzi, R. Hlushchuk, V. Djonov, A. H. Zisch, J. A. Hubbell, F. E. Weber, M. P. Lutolf, Enzymatic formation of modular cell-instructive fibrin analogs for tissue engineering. *Biomaterials* **28**, 3856–3866 (2007).
67. Y. Yang, U. Khoe, X. Wang, A. Horii, H. Yokoi, S. Zhang, Designer self-assembling peptide nanomaterials. *Nano Today* **4**, 193–210 (2009).
68. R. V. Ulijn, A. M. Smith, Designing peptide based nanomaterials. *Chem. Soc. Rev.* **37**, 664–675 (2008).
69. J. Boekhoven, S. I. Stupp, 25th anniversary article: Supramolecular materials for regenerative medicine. *Adv. Mater.* **26**, 1642–1659 (2014).
70. J. D. Hartgerink, E. Beniash, S. I. Stupp, Peptide-amphiphile nanofibers: A versatile scaffold for the preparation of self-assembling materials. *Proc. Natl. Acad. Sci. U.S.A.* **99**, 5133–5138 (2002).
71. Z. Yang, X. Zhao, A 3D model of ovarian cancer cell lines on peptide nanofiber scaffold to explore the cell-scaffold interaction and chemotherapeutic resistance of anticancer drugs. *Int. J. Nanomedicine* **6**, 303–310 (2011).
72. A. Guzman, M. J. Ziperstein, L. J. Kaufman, The effect of fibrillar matrix architecture on tumor cell invasion of physically challenging environments. *Biomaterials* **35**, 6954–6963 (2014).
73. B. Geiger, A. Bershadsky, R. Pankov, K. M. Yamada, Transmembrane crosstalk between the extracellular matrix and the cytoskeleton. *Nat. Rev. Mol. Cell Biol.* **2**, 793–805 (2001).
74. M. P. Carvalho, E. C. Costa, S. P. Miguel, I. J. Correia, Tumor spheroid assembly on hyaluronic acid-based structures: A review. *Carbohydr. Polym.* **150**, 139–148 (2016).
75. X. Xu, L. A. Gurski, C. Zhang, D. A. Harrington, M. C. Farach-Carson, X. Jia, Recreating the tumor microenvironment in a bilayer, hyaluronic acid hydrogel construct for the growth of prostate cancer spheroids. *Biomaterials* **33**, 9049–9060 (2012).
76. A. E. G. Baker, R. Y. Tam, M. S. Shoichet, Independently tuning the biochemical and mechanical properties of 3D hyaluronan-based hydrogels with oxime and Diels–Alder chemistry to culture breast cancer spheroids. *Biomacromolecules* **18**, 4373–4384 (2017).
77. M. Chau, S. E. Sriskandha, H. Thérien-Aubin, E. Kumacheva, Supramolecular nanofibrillar polymer hydrogels. *Adv. Polym. Sci.* **268**, 167–208 (2015).
78. P. P. Provenzano, D. R. Inman, K. W. Eliceiri, J. G. Knittel, L. Yan, C. T. Rueden, J. G. White, P. J. Keely, Collagen density promotes mammary tumor initiation and progression. *BMC Med.* **6**, 11 (2008).
79. K. R. Levental, H. Yu, L. Kass, J. N. Lakin, M. Egeblad, J. T. Emler, S. F. T. Fong, K. Csizsar, A. Giaccia, W. Weninger, M. Yamauchi, D. L. Gasser, V. M. Weaver, Matrix crosslinking forces tumor progression by enhancing integrin signaling. *Cell* **139**, 891–906 (2009).
80. Y. Liang, J. Jeong, R. J. DeVolder, C. Cha, F. Wang, Y. W. Tong, H. Kong, A cell-instructive hydrogel to regulate malignancy of 3D tumor spheroids with matrix rigidity. *Biomaterials* **32**, 9308–9315 (2011).
81. A. M. Oelker, S. M. Morey, L. G. Griffith, P. T. Hammond, Helix versus coil polypeptide macromers: Gel networks with decoupled stiffness and permeability. *Soft Matter* **8**, 10887–10895 (2012).
82. Y. S. Schifffenbauer, R. Abramovitch, G. Meir, N. Nevo, M. Holzinger, A. Itin, E. Keshet, M. Neeman, Loss of ovarian function promotes angiogenesis in human ovarian carcinoma. *Proc. Natl. Acad. Sci. U.S.A.* **94**, 13203–13208 (1997).
83. D. R. Griffin, A. M. Kasko, Photodegradable macromers and hydrogels for live cell encapsulation and release. *J. Am. Chem. Soc.* **134**, 13103–13107 (2012).
84. A. Blanz, R. Verber, O. O. Mykhaylyk, A. J. Ryan, J. Z. Heath, C. W. I. Douglas, S. P. Armes, Sterilizable gels from thermoresponsive block copolymer worms. *J. Am. Chem. Soc.* **134**, 9741–9748 (2012).
85. S. Kessel, C. N. Urbani, M. J. Monteiro, Mechanically driven reorganization of thermoresponsive diblock copolymer assemblies in water. *Angew. Chem. Int. Ed. Engl.* **50**, 8082–8085 (2011).

86. H. Thérien-Aubin, Y. Wang, K. Nothdurft, E. Prince, S. Cho, E. Kumacheva, Temperature-responsive nanofibrillar hydrogels for cell encapsulation. *Biomacromolecules* **17**, 3244–3251 (2016).
87. J. M. Heffernan, D. J. Overstreet, S. Srinivasan, L. D. Le, B. L. Vernon, R. W. Siriani, Temperature responsive hydrogels enable transient three-dimensional tumor cultures via rapid cell recovery. *J. Biomed. Mater. Res. A* **104A**, 17–25 (2016).
88. D. Wang, D. Cheng, Y. Guan, Y. Zhang, Thermoreversible hydrogel for in situ generation and release of HepG2 spheroids. *Biomacromolecules* **12**, 578–584 (2011).
89. F. Pampaloni, E. G. Reynaud, E. H. K. Stelzer, The third dimension bridges the gap between cell culture and live tissue. *Nat. Rev. Mol. Cell Biol.* **8**, 839–845 (2007).
90. J. Friedrich, C. Seidel, R. Ebner, L. A. Kunz-Schughart, Spheroid-based drug screen: Considerations and practical approach. *Nat. Protoc.* **4**, 309–324 (2009).
91. K. H. Lee, D. Y. No, S.-H. Kim, J. H. Ryoo, S. F. Wong, S.-H. Lee, Diffusion-mediated in situ alginate encapsulation of cell spheroids using microscale concave well and nanoporous membrane. *Lab Chip* **11**, 1168–1173 (2011).
92. B. Kwak, A. Ozelikkale, C. S. Shin, K. Park, B. Han, Simulation of complex transport of nanoparticles around a tumor using tumor-microenvironment-on-chip. *J. Control. Release* **194**, 157–167 (2014).
93. H. F. Chan, Y. Zhang, Y.-P. Ho, Y.-L. Chiu, Y. Jung, K. W. Leong, Rapid formation of multicellular spheroids in double-emulsion droplets with controllable microenvironment. *Sci. Rep.* **3**, 3462 (2013).
94. A. Y. Hsiao, Y.-C. Tung, C.-H. Kuo, B. Mosadegh, R. Bedenis, K. J. Pienta, S. Takayama, Micro-ring structures stabilize microdroplets to enable long term spheroid culture in 384 hanging drop array plates. *Biomed. Microdevices* **14**, 313–323 (2012).
95. Y.-C. Tung, A. Y. Hsiao, S. G. Allen, Y.-s. Torisawa, M. Ho, S. Takayama, High-throughput 3D spheroid culture and drug testing using a 384 hanging drop array. *Analyst* **136**, 473–478 (2011).
96. O. Frey, P. M. Misun, D. A. Fluri, J. G. Hengstler, A. Hierlemann, Reconfigurable microfluidic hanging drop network for multi-tissue interaction and analysis. *Nat. Commun.* **5**, 4250 (2014).
97. B. Patra, Y.-H. Chen, C.-C. Peng, S.-C. Lin, C.-H. Lee, Y.-C. Tung, A microfluidic device for uniform-sized cell spheroids formation, culture, harvesting and flow cytometry analysis. *Biomicrofluidics* **7**, 054114 (2013).
98. B. Patra, C.-C. Peng, W.-H. Liao, C.-H. Lee, Y.-C. Tung, Drug testing and flow cytometry analysis on a large number of uniform sized tumor spheroids using a microfluidic device. *Sci. Rep.* **6**, 21061 (2016).
99. P. Sabhachandani, V. Motwani, N. Cohen, S. Sarkar, V. Torchilin, T. Konry, Generation and functional assessment of 3D multicellular spheroids in droplet based microfluidics platform. *Lab Chip* **16**, 497–505 (2016).
100. A. Y. Hsiao, Y.-s. Torisawa, Y.-C. Tung, S. Sud, R. S. Taichman, K. J. Pienta, Microfluidic system for formation of PC-3 prostate cancer co-culture spheroids. *Biomaterials* **30**, 3020–3027 (2009).
101. L. Y. Wu, D. Di Carlo, L. P. Lee, Microfluidic self-assembly of tumor spheroids for anticancer drug discovery. *Biomed. Microdevices* **10**, 197–202 (2008).
102. S. V. Murphy, A. Atala, 3D bioprinting of tissues and organs. *Nat. Biotechnol.* **32**, 773–785 (2014).
103. S. Nath, G. R. Devi, Three-dimensional culture systems in cancer research: Focus on tumor spheroid model. *Pharmacol. Ther.* **163**, 94–108 (2016).
104. K.-V. Nguyen-Ngoc, K. J. Cheung, A. Brenot, E. R. Shamir, R. S. Gray, W. C. Hines, P. Yaswen, Z. Werb, A. J. Ewald, ECM microenvironment regulates collective migration and local dissemination in normal and malignant mammary epithelium. *Proc. Natl. Acad. Sci. U.S.A.* **109**, E2595–E2604 (2012).
105. J. N. Beck, A. Singh, A. R. Rothenberg, J. H. Elisseeff, A. J. Ewald, The independent roles of mechanical, structural and adhesion characteristics of 3D hydrogels on the regulation of cancer invasion and dissemination. *Biomaterials* **34**, 9486–9495 (2013).
106. K. M. Tevis, Y. L. Colson, M. W. Grinstaff, Embedded spheroids as models of the cancer microenvironment. *Adv. Biosyst.* **1**, 1700083 (2017).
107. D. Yip, C. H. Cho, A multicellular 3D heterospheroid model of liver tumor and stromal cells in collagen gel for anti-cancer drug testing. *Biochem. Biophys. Res. Commun.* **433**, 327–332 (2013).
108. W. Zhang, C. Li, B. C. Baguley, F. Zhou, W. Zhou, J. P. Shaw, Z. Wang, Z. Wu, J. Liu, Optimization of the formation of embedded multicellular spheroids of MCF-7 cells: How to reliably produce a biomimetic 3D model. *Anal. Biochem.* **515**, 47–54 (2016).
109. C. R. I. Lam, H. K. Wong, S. Nai, C. K. Chua, N. S. Tan, L. P. Tan, A 3D biomimetic model of tissue stiffness interface for cancer drug testing. *Mol. Pharm.* **11**, 2016–2021 (2014).
110. X. Xu, C. R. Sabanayagam, D. A. Harrington, M. C. Farach-Carson, X. Jia, A hydrogel-based tumor model for the evaluation of nanoparticle-based cancer therapeutics. *Biomaterials* **35**, 3319–3330 (2014).
111. B. Kim, G. Han, B. J. Toley, C.-k. Kim, V. M. Rotello, N. S. Forbes, Tuning payload delivery in tumour cyndroids using gold nanoparticles. *Nat. Nanotechnol.* **5**, 465–472 (2010).
112. H.-F. Tsai, A. Trubelja, A. Q. Shen, G. Bao, Tumour-on-a-chip: Microfluidic models of tumour morphology, growth and microenvironment. *J. R. Soc. Interface* **14**, 20170137 (2017).
113. P. M. Valencia, O. C. Farokhzad, R. Karnik, R. Langer, Microfluidic technologies for accelerating the clinical translation of nanoparticles. *Nat. Nanotechnol.* **7**, 623–629 (2012).
114. A. Albanese, A. K. Lam, E. A. Sykes, J. V. Rocheleau, W. C. W. Chan, Tumour-on-a-chip provides an optical window into nanoparticle tissue transport. *Nat. Commun.* **4**, 2718 (2013).
115. O. Chaudhuri, L. Gu, M. Darnell, D. Klumpers, S. A. Bencherif, J. C. Weaver, N. Huebsch, D. J. Mooney, Substrate stress relaxation regulates cell spreading. *Nat. Commun.* **6**, 6364 (2015).
116. W. Li, S. Lee, M. Ma, S. M. Kim, P. Guye, J. R. Pancoast, D. G. Anderson, R. Weiss, R. T. Lee, P. T. Hammond, Microbead-based biomimetic synthetic neighbors enhance survival and function of rat pancreatic β -cells. *Sci. Rep.* **3**, 2863 (2013).
117. P. P. Provenzano, K. W. Eliceiri, J. M. Campbell, D. R. Inman, J. G. White, P. J. Keely, Collagen reorganization at the tumor-stromal interface facilitates local invasion. *BMC Med.* **4**, 38 (2006).
118. M. W. Conklin, J. C. Eickhoff, K. M. Ricking, C. A. Pehlke, K. W. Eliceiri, P. P. Provenzano, A. Friedl, P. J. Keely, Aligned collagen is a prognostic signature for survival in human breast carcinoma. *Am. J. Pathol.* **178**, 1221–1232 (2011).
119. A. Birgersdotter, R. Sandberg, I. Ernberg, Gene expression perturbation in vitro—A growing case for three-dimensional (3D) culture systems. *Semin. Cancer Biol.* **15**, 405–412 (2005).
120. J. Lee, S. Kotliarova, Y. Kotliarov, A. Li, Q. Su, N. M. Donin, S. Pastorino, B. W. Purov, N. Christopher, W. Zhang, J. K. Park, H. A. Fine, Tumor stem cells derived from glioblastomas cultured in bFGF and EGF more closely mirror the phenotype and genotype of primary tumors than do serum-cultured cell lines. *Cancer Cell* **9**, 391–403 (2006).
121. R. L. Ochs, J. Fensterer, N. P. Ohori, A. Wells, M. Gabrin, L. D. George, P. Kornblith, Evidence for the isolation, growth, and characterization of malignant cells in primary cultures of human tumors. *In Vitro Cell. Dev. Biol. Anim.* **39**, 63–70 (2003).
122. H. Clevers, Modeling development and disease with organoids. *Cell* **165**, 1586–1597 (2016).
123. N. Gjorevski, N. Sachs, A. Manfrin, S. Giger, M. E. Bragina, P. Ordóñez-Morán, H. Clevers, M. P. Lutolf, Designer matrices for intestinal stem cell and organoid culture. *Nature* **539**, 560–564 (2016).

Acknowledgments: We thank A. McGuigan, D. Cescon, and A. Eitan for the fruitful discussions. **Funding:** We thank the Natural Sciences and Engineering Research Council of Canada (NSERC) (Discovery Grants) for financial support of this work. E.K. is the Canada Research Chair (Tier 1) in Advanced Polymer Materials. Y.L. acknowledges the Banting Postdoctoral Fellowship program (NSERC Canada). **Author contributions:** Y.L. and E.K. wrote the draft. **Competing interests:** The authors declare that they have no competing interests. **Data and materials availability:** All data needed to evaluate the conclusions in the paper are present in the paper. Additional data related to this paper may be requested from the authors.

Submitted 3 January 2018

Accepted 13 March 2018

Published 27 April 2018

10.1126/sciadv.aas8998

Citation: Y. Li, E. Kumacheva, Hydrogel microenvironments for cancer spheroid growth and drug screening. *Sci. Adv.* **4**, eaas8998 (2018).